

RELATIVE PERMEABILITY EXPERIMENTS MONITORED BY NMR

P.O. Mangane, G. Dubes, B. Nicot

Total

This paper was prepared for presentation at the International Symposium of the Society of Core Analysts held in Vienna, Austria, 27 August – 1 September 2017

ABSTRACT

Executing successful waterflood recovery projects in field requires prior laboratory core flooding studies, in order to better understand fluid displacement and to predict the recovery efficiency. When dealing with reservoir rocks that display complex fluid distribution (due to pore size heterogeneity, capillary end effect, wettability heterogeneity ...), the use of technique with a strong imaging capacity is crucial to evaluate the flow characteristics. Traditionally, fluid saturation changes during core floods are monitored using X-Rays. However, the use of dopants is usually required in order to improve the density contrast between fluids. These dopants could alter the wettability of the rock or could chemically inhibit some EOR operations, such as low salt salinity injection for example.

In this work, we conduct core flooding tests using NMR as monitoring tool on a D₂O brine/oil/rock system. Previous works evidenced that NMR is promising for monitoring core flood experiments, due to its sensitivity to volume, fluid saturation, pore size and wettability. Saturation variation and wettability change can be captured by a T₂ experiment. As D₂O has no NMR signal, its use avoids adding dopants. Running other specific NMR pulse sequences, the fluid distribution within the rock can be computed either in bulk (e.g. saturation profile) or per pore size class (e.g. spatial T₂). This spatially resolved T₂ can be useful in systems that display complex fluid distribution, due to its pore size heterogeneity. To apply this monitoring technique, imbibition experiments were conducted on a low-field spectrometer into oil saturated outcrop plugs, bumping successively the flow rate to reduce the capillary end effects. In association with NMR data, relative permeability simulation was computed to determine the residual saturations and to better evaluate the fluid displacement efficiency during the water injection. Compared to traditional methods like X-ray techniques, the use of NMR to monitor water-flooding experiments can provide further understanding of flow mechanisms, especially in complex carbonate systems such as carbonate.

INTRODUCTION

Relative Permeability data are commonly determined in laboratory from dynamic displacement tests such as coreflood experiments based on unsteady or steady

techniques[1][2] [3]. The coreflood experiments provide principally two time-dependent flow data - the pressure differential across the sample and the volume of displaced fluid recovered, and define the end-point effective permeability (i.e. effective permeability at S_{wi} and at S_{or}). Then, an automated tool (e.g. CYDARTM) can be used to numerically calculate the corresponding relative permeability curve [3], adjusting specific K_r and P_c models until they reproduce the volume of oil recovered and the pressure drop (i.e. the past behavior): history matching.

Corefloods tests can be monitored using gamma/X-Rays techniques which enable measuring local saturations and more importantly visualizing saturation profiles as a function of core length during the flood[4]. This powerful monitoring technique is commonly used in the core analysis domain. However, it has a significant drawback due to the need of doping one phase (e.g. usually Sodium Iodide or Cesium Chloride for the water and/or iododecane for the oil phase). Actually, add dopants allow increasing the difference in attenuation between fluids saturating the core sample, then improving the accuracy of the saturation measurements. When studying the effect of low salinity brines for example, the addition of dopant is not recommended as it is suspected to potentially alter the wettability of the rock during the coreflooding test; therefore dopant could considerably change the fluid displacement (i.e. relative permeability – K_r) efficiency during the waterflooding experiment.

Recent published works showed that NMR technology is an alternative to monitor fluid displacement in the laboratory and in the well too[5][6][7][8][9]. They evidenced that NMR is quite promising, due to its sensitivity to volume, fluid saturation, pore size, wettability, and particularly due to its strong imaging capacity[9]. Another advantage of NMR for monitoring corefloods is the possibility of using a common physic of measurements at multiple scales (i.e. lab scale and well scale). J Mitchell *et al.* [5] and A Al-Yaarabi *et al.*, [8] have determined oil and brine saturation change during the flood and estimated the final remaining oil distribution, by conducting in-situ measurements of oil and brine saturations during laboratory corefloods on a low-field bench-top NMR magnet with a defined fluid injection sequence, using diffusion and relaxation measurements. Furthermore, they displayed non-uniform oil saturation during the EOR process from spatially resolved T_2 analysis. In this study, the obtained saturations values are shown to be in quantitative agreement with gravimetric measurements of recovered oil, displaying the accuracy and reliability of the NMR data. Arora *et al.* [7] performed a downhole rock flooding experiment from a micropilot single-well in situ EOR evaluation. They estimated the saturation change across the flood zone from the partitioning of the porosity map scaled in relaxation versus diffusion. Washburn and Madelin [9] have shown the strong capacity of imaging multiphase fluid saturation via sodium NMR. All these studies demonstrate the high potential of the NMR technique for monitoring multiphase flow, in terms of saturation change quantification and visualization of the fluid phase distribution during multiphase flow.

In this study, two unsteady-state imbibition experiments were performed on a low-field DRX spectrometer (MARAN DRX2-HF from Oxford ltd) in an attempt to constrain the computation of relative permeabilities with the NMR derived saturation profiles within

core at key stages of the waterflood. This paper begins with a brief description of the involved cored plugs and fluids. Next, in the experimental section, we describe the way to set the irreducible water saturation, Swirr and wettability state of the core samples. The experimental setup and protocol used for performing the waterflood tests are also described. We finally discuss the potential of NMR to monitor a coreflood experiment for Kr calculation, by analyzing the acquired flow and NMR data.

SAMPLES

Fluids

- **Crude oil and Synthetic oil**

At 25°C, the used crude oil has a density ρ of 0.864 g/cm³ and a viscosity μ of 20.92 cP. The synthetic one was a mineral oil, Marcol 52, manufactured by ExxonMobil. At 25°C, Marcol 52 has a density ρ of 0.830 g/cm³ and a viscosity μ of 12.2 cP.

- **Synthetic brine**

The synthetic brine used for establishing the initial water saturation Swirr and for the waterflood experiments consisted in heavy water (i.e. D₂O) with dissolved salts (see Table 1) at 70 g/l salinity. In addition to major elements (i.e. Na and Cl), this brine was also composed of divalent cations (i.e. Ca²⁺).

NaCl	CaCl ₂	Density, ρ , at 25 °C	Viscosity, μ , at 25 °C
mol/l	mol/l	g/cc	cP
0.40	0.33	1.148	0.8

Table 1. Chemical composition of the synthetic brine used in the waterflood tests.

The interest of using such brine is twofold:

1. According to Shabib-Asl et al., [10], using divalent ions on top of NaCl, has been referred to assist in adsorption of oil onto the surfaces of rock (i.e. favoring the core to become oil wet during the aging step).
2. The use of D₂O is an experimental trick. Actually, heavy water (i.e. D₂O brine) has no NMR signal and was consequently used to prevent adding dopants, in order to discriminate oil from water in the NMR experiment. Only the oil phase will be visible to NMR, using D₂O.

Core plugs

For the waterflood tests, quarried outcrop plugs were used, instead of actual reservoir rocks: Bentheimer sandstone and Sireuil carbonate. Figure 1 presents the 1D T₂ distributions (top) and the oil volume profile (bottom) acquired on both plugs 100% saturated in “normal” brine (i.e. the same synthetic brine described above, with H₂O instead of D₂O). The T₂ distributions display a single pore size class (i.e. unimodal T₂ distribution) for Bentheimer Sandstone and a bimodal porosity (i.e. Bimodal T₂

distribution) for Sireuil carbonate, respectively. The NMR profiles at 100% S_w appear relatively flat for the two samples, indicating that the cores are homogeneous in terms of porosity. Both core plugs were cylindrically sampled to dimensions of 38 mm in diameter and 50 mm in length. The characteristics of both samples are reported in Table 2.

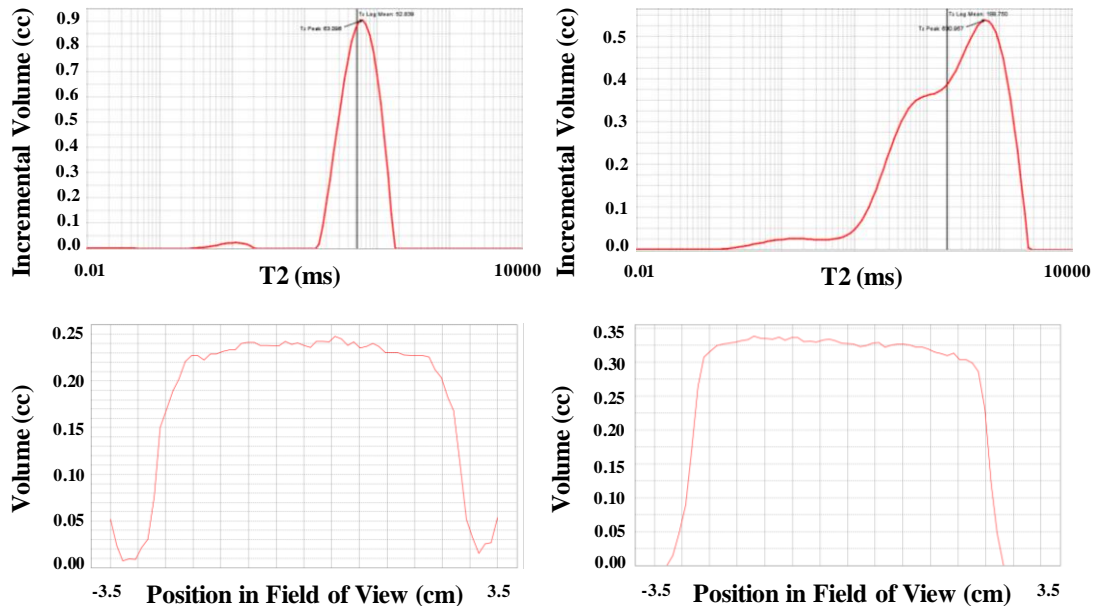


Figure 1 1D T2 distribution (top) and NMR profile along core (bottom), on 100% water saturated plug for Bentheimer (left) and Sireuil (right).

Sample	ϕ (p.u)	K (mD)	PV (cc)	$Swirr$ (frac)
BEN	26.2	2000	14.80	0.09
SIR	29.0	978.8	16.36	0.10

Table 2. Characteristics of core sample used in the waterflood tests

EXPERIMENTAL

Core preparation

Prior to the saturation state, plugs were cleaned during four days at a temperature of 60 °C, using chloroform then isopropanol. After that, plugs were dried at 80 °C during 48 hours, then placed under vacuum and saturated with synthetic brine under pressure.

- **Setting Swirr**

The brine-saturated plugs were flooded by viscous displacement with crude oil under confining pressure, $P_{conf} = 65$ bars, to provide an initial oil saturation.

To ensure obtaining a homogeneous initial oil saturation along the core, the viscous displacements were successively conducted in both directions along the core length. A graduated tube at the outlet, collecting the effluents, allowed monitoring the variation of the average water saturation from material balance.

- **Ageing step**

The core plugs at irreducible water, S_{wirr} , were aged statically under crude oil during 3 weeks at 80 °C, in an attempt to change the rock surface wettability from initially water-wet to oil-wet. This test was performed at 80°C, under 65 bars of confining pressure and 20 bars of pore pressure. This 20 bars pore pressure were maintained into the core plug, in order to prevent, at the ageing temperature, gas bubble formation from the crude oil and fluids evaporation. To prevent the establishment of wettability gradients along the core, the crude oil was renewed once per week by viscous displacement, successively following the two different directions along the core length (i.e. one pore volume PV per direction, successively). This was performed at flowrate slightly lower than the one for the S_{wirr} setting, to prevent an additional water production.

At the end of the aging step, the crude oil was replaced by flooding it with toluene, followed by synthetic oil (Marcol 52). This mineral oil injection viscous was also performed at flowrate below the one for the S_{wirr} setting.

NMR Hardware and measurements

The NMR system (MARAN DRX2-HF from Oxford ltd) consists in a 2MHz low-field DRX spectrometer, equipped with magnetic field gradients on the vertical axis. Two sets of NMR data were acquired during these experimental studies, at different saturation states and especially at different strategic times according to the acquisition duration of the different NMR pulse sequences:

- 1D saturation profile (needed for the history matching of the K_r curve and 1D T_2 relaxation times distribution were acquired during all the core flooding tests, due to their short acquisition time (i.e. between 20 minutes to 2 hours, depending on the oil saturation – the lower the oil saturation, the longer the acquisition time) and for their high interest in monitoring the saturation variation.
- Spatially resolved T_2 relaxation time map was run at the end of each flow rate step. The strategy of these acquisitions is to quantify the saturation profile of each pore size class after each flow rate step. This acquisition can take between 3 hours to 10 hours and the flow rate step can take up to 5 hours.

Waterflood experimental set up

The core flooding tests were conducted using an NMR compatible core holder, manufactured by Deadalus Innovations. This core holder consists of an overburden core cell equipped with dual port end plugs; one port for injecting fluids and a second for measuring the pressure drop across the core plug, which is required for K_r estimation. Collected at the outlet into a graduated tube, the produced volumes were continuously weighted and monitored using a high resolution camera. This setup was put into place to capture the volume of displaced oil recovered, which is an important input data for K_r computation. Note that the production from gravimetric data (i.e. volume from weigh data – see section oil production computation) was considered as the reference and its quality was punctually controlled with volumes measured from the image of the outlet

tube. To calculate the produced oil volume, from weigh data, we had to consider separately distinct block times according to the nature (i.e. density) of the effluent fluids: 1) Time before breakthrough, where only Marcol was produced; 2) Time after breakthrough, where effluents consist of both Marcol and brine.

Core flood protocol

The core plug, saturated with Marcol at Swirr, was vertically mounted under confining pressure (i.e. 65 bars) into the core holder. Flooding fluids were injected, at room temperature, from below using a dual piston pump to maintain constant flow rate. Prior carrying out the waterflood, the end-point effective oil permeability at irreducible water saturation ($K_o @Swirr$) was determined, by injecting the synthetic oil at several flow rates and measuring their corresponding ΔP . Then, the water injection was conducted at low rate (i.e. capillary number $Nc \sim 10^{-7}$, Table 3). This first low flow rate was maintained until the cumulative oil production stabilized. Commonly in coreflood experiments, capillary end effects arise at the outlet of the core sample from the discontinuity of capillarity in the wetting phase (i.e. build up of the wetting phase at the outlet of the sample). This important issue can artificially reduce the relative permeability to water, particularly in the oil-wet case for a rock/water/oil system [3]. Traditionally, high flow rates are used to reduce capillary effects. Thus, the flow rate was successively bumped several times, until reaching the residual oil saturation, S_{or} . At each bump, the new flow rate is maintained constant until the stabilization of the resulting cumulative oil production. At the end of the last flow rate step, the end-point effective permeability at residual oil saturation ($K_w @S_{or}$ - The final point of a water flood) was determined, by injecting the synthetic brine at several flow rate steps (lower or equal to the final Q) and measuring the corresponding ΔP .

RESULTS AND DISCUSSIONS

As previously mentioned, the setting of the initial saturations and both water-flood tests were performed using heavy water. Thus, all the resulting 1D and 2D NMR distributions presented here, from the Swirr state to the S_{or} state, display uniquely the oil signal (from Figure 2 to Figure 4), since D_2O has no NMR signal.

For the bimodal core (Sireuil), it is worth noticing that the oil localization in the pore space was determined at initial oil saturation $S_{o_{init}}$, (i.e. state prior to the water flood) from the 1D T_2 distributions and the spatial T_2 maps (Figure 2 and Figure 3): with an $S_{o_{init}} = 90\%$, the oil volume was located in both the big pores (i.e. 90%-95% of the $S_{o_{init}}$) and the small pores (i.e. 5%-10% of the $S_{o_{init}}$).

The waterflood tests were conducted, from $S_{o_{init}}$, injecting a volume of synthetic brine equal to 11 PV and 8.2 PV in the core plug for Bentheimer and Sireuil, respectively (the PV of water injected at each flood stage are presented in Table 3).

Bentheimer Sandstone				Sireuil Carbonate			
Flow rate, Q	Nc	Injected PV	ROS	Flow rate, Q	Nc	Injected PV	ROS
c/h		cc	frac	cc/h		PVI	frac
2	3,69E-08	2,3	0,19	0,5	8,38E-09	0,7	0,75
6	1,11E-07	1,7	0,18	2,2	3,69E-08	3,1	0,56
12	2,22E-07	2,5	0,17	4,5	7,55E-08	2,4	0,46
24	4,43E-07	4,5	0,16	6	1,01E-07	2,1	0,36

Table 3. Capillary number N_c , Number of pore volume PV injected and remaining oil saturation ROS, at each flood stage

Notice that NMR measurements, particularly the oil volume profile along core length needed for K_r history matching, could not be acquired during the test performed on the Bentheimer sandstone. This was due to a technical issue. Thus, proper NMR could be only obtained before and after the imbibition experiment, when the flooding was stopped. Afterward, this issue was fixed by improving our experimental setup. This has allowed acquiring in-situ NMR profiles at each stage of the flood, during the test on the Sireuil carbonate.

NMR results

In Figure 2 we present the T_2 distributions and 1D NMR profiles obtained at irreducible water saturation (S_{wirr}) and at the end of each flow rate step for both Bentheimer and Sireuil samples. On both samples, the 1D T_2 distributions highlighted a decrease in oil saturation from the $S_{o_{init}}$ to remaining oil saturation (Table 3), during the waterflood. The ROS (e.g. Average remaining oil saturation, including the end effect) was evaluated to be 15.5% and 36% for the Bentheimer sandstone and the Sireuil carbonate, respectively. Moreover, the position of the T_2 peak remained unchanged during all the brine injections, denoting that there was no wettability alteration during both the waterflood tests. For the bimodal carbonate (Sireuil), the T_2 distributions show that the oil was recovered from the big pores ($90 \text{ ms} < T_2$) as well as from the small pores ($T_2 < 90 \text{ ms}$). Figure 2 also reports the NMR saturations profiles consisting in the stack of individual oil volume profiles by slice along the core, compared to linear X-ray scanning technique where saturation profiles are often taken in a section along the axis of the cylinder. This allows capturing all the pore heterogeneity along the core, typically when dealing with complex rocks such as the bimodal Sireuil carbonate. In addition to the oil saturation decrease (Table 3), the NMR profile has also evidenced an end effect at the outlet of both samples (Figure 2). This discontinuity is present over the last 0.6 cm for the Bentheimer and 1.5 cm for Sireuil sample. This difference can be attributed either to the difference in the applied N_c (Table 3) or to wettability. An interpretation in term of wettability can be made between both tests only with equal N_c .

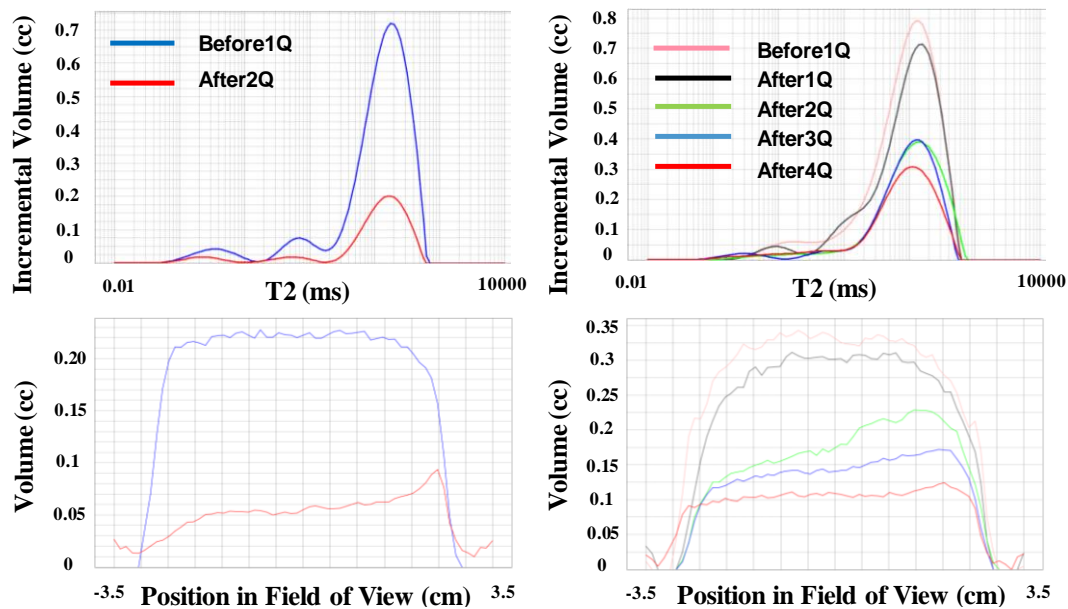


Figure 2 T₂ distribution (top) and oil volume profiles (bottom) at each flood stage (Q corresponding to flow rate step), for Bentheimer (left) and Sireuil (right).

Figure 3 presents the spatially resolved T₂ relaxation time maps obtained at irreducible water saturation (Swirr) and after each flow step for both samples. These measurements provide a partitioning of the porosity map scaled in relaxation (x-axis) versus saturation profile (z-axis). Moreover, individual T₂ distributions by slice along the core can be generated from these maps, allowing the localization of the remaining oil in space (z-axis) and pore size (T₂ axis). On both samples, the spatial T₂ maps and the individual T₂ stack show:

- A decrease of the oil volume during the waterflood (Table 3).
- The resulting capillary end effect at the outlets (Figure 3).
- Oil volume change into the small and big pores, for the Sireuil carbonate.

Figure 4 illustrates the total oil volume profile along the Sireuil sample, the saturation profiles for the small pores (T₂<90ms) and the big pores (T₂>90ms) at each stage of the waterflood, evaluated from the spatially resolved T₂ maps. This partitioning of the porosity allows evaluating the oil saturation change in each pore class. It confirms the decrease of the oil volume in both small and large pores. Moreover, both pore size classes display an end effect at the outlet of the sample. Surprisingly, non-uniform oil saturation is evidenced in both pore size classes prior to the water injection (black profiles in Figure 4). This non-uniformity seems to disappear during the flooding. Probably, this could have occurred during the setting of the initial saturation by drainage or during the ageing phase (wettability gradient into the small pores). This phenomenon will be investigated in more details in the future. However, the observation of this saturation gradient into the different pore size groups is specific to NMR and could not have been observed using the X-ray technique.

Oil Recovery

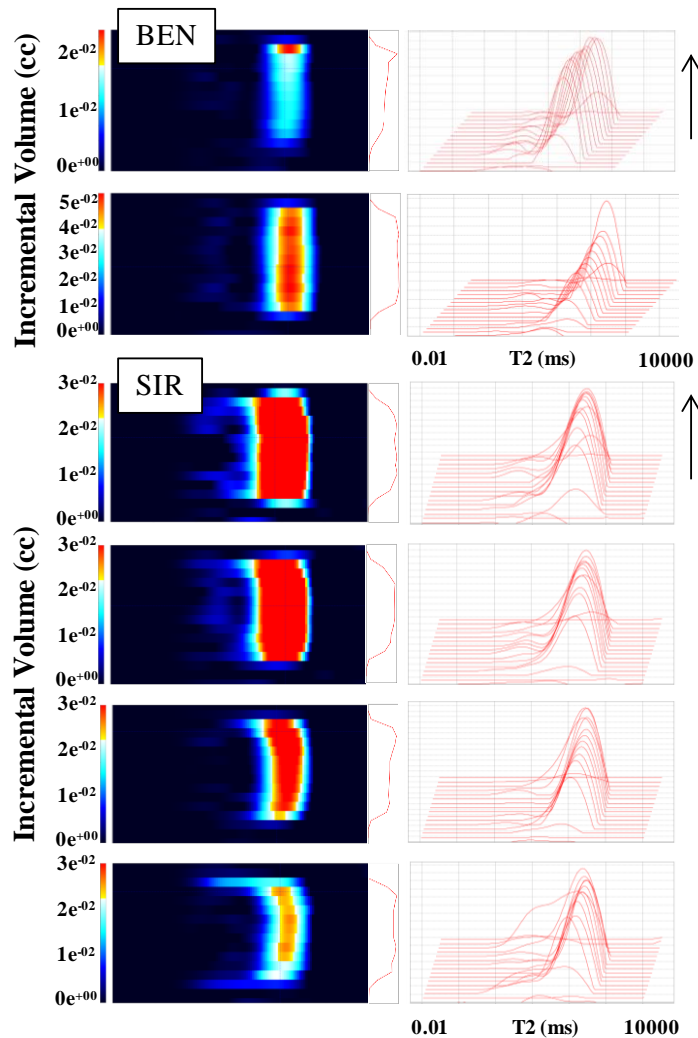


Figure 3 Spatial T₂ at each stage of the waterflood test. Arrows indicate direction of flow, for Bentheimer sandstone (top) and Sireuil carbonate (bottom).

The oil production curves of both samples are reported in Figure 5. Comparing both curves, the Bentheimer sandstone appears more “water-wet” than the Sireuil carbonate. Actually, the behaviour of the carbonate core is characterized by earlier breakthrough where more than 80% of the oil recovery has occurred from the flow rate bumps. On the other hand, the sandstone core exhibits a later breakthrough where most of the recovery happens before breakthrough (i.e. more than 90% of the oil recovery has appeared during the first flow rate step).

The presence of end effects at the outlet of both samples evidences (Figure 2) that the crude oil ageing has rendered the cores less water wet than they were initially.

K_r computation

The relative permeability behavior of the waterflood tests was computed by history matching, from CYDAR™ using experimental data (i.e. Volume of oil recovered and pressure drop) and some analytical functions for relative permeability (i.e. LET function) and capillary pressure curve (i.e. Logbeta function). Actually, no experimental *P_c* data is available for both tests. The history matching of *K_r* and *P_c* curves is performed by optimizing the parameters for *K_r* and *P_c*. The optimization adjusts these models until they reproduce the experimental data.

About the saturation profile data, the purpose is not to get a perfect match with the experimental data, but to drive the *K_r* computation with a capillary pressure as realistic as possible. Note that the NMR and the gravimetric saturation measurements agree within 5

saturation units (s.u) at maximum (Figure 6). In both imbibition tests, the simulated oil recoveries reproduce the input experimental data (Figure 5).

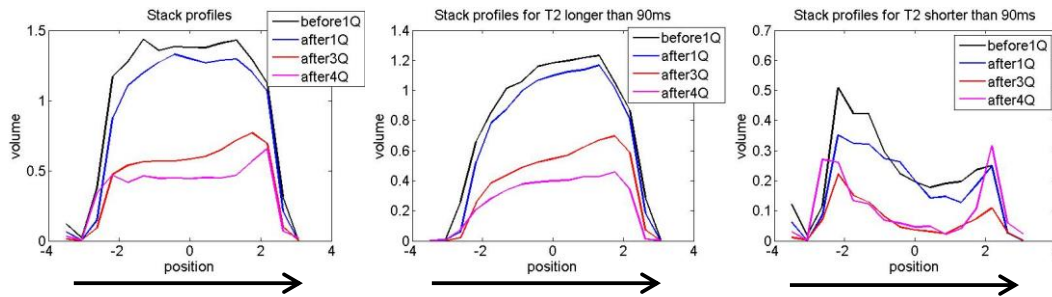


Figure 4 **Sireuil carbonate**: Oil volume profile deduced from the Spatial T_2 maps, at each stage of the waterflood. From left to right, total NMR profile, NMR profile of the big and small pores. Arrows indicate direction of flow.

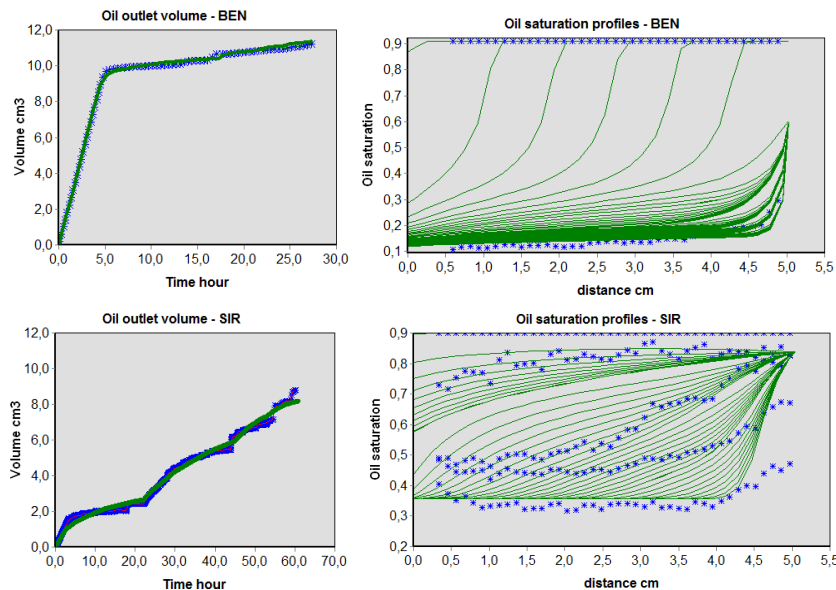


Figure 5 Volume of oil recovered and NMR saturation profile for Bentheimer sandstone (top) and Sireuil carbonate (bottom) – Experimental data in blue and simulated data in green.

P_c would have been better constrained by experimental data. Unfortunately, this data was not available.

As observed on the experimental data, the simulated end effect at the outlet face appeared

more pronounced for the Sireuil carbonate (simulated $R_{os} = 36\%$ to 80%) than for the Bentheimer sandstone (simulated $R_{os} = 15\%$ to 50%). This can be attributed either to the oil-wet nature or to the bimodality of the Sireuil carbonate. In this paper we present only the K_r computation on the homogeneous Bentheimer sandstone. The difficulty of computing K_r curves in the case of heterogeneous such as Sireuil carbonate is out of the scope of this paper.

Reported in Figure 6, the two simulated K_r curves (i.e. K_{ro} and K_{rw} , determined using Corey model) on the Bentheimer sandstone display a shape relatively soft where the water relative permeability K_{rw} appears relatively low at high water saturations: K_r cross-point is $>50\%$ S_w , $K_{rw}(S_{or})$ around 0.15 and the alpha coefficients are 2.1 and 3.6 for the K_{ro} and K_{rw} , respectively. The fractional flow curve (described by Buckley and Levrett [11] and extended by Welge [12], Figure 6), deduced from the K_r curve, exhibits

a late critical water saturation (saturation above which the water becomes mobile). This behavior indicates the water-wet nature of the sandstone and confirms the late breakthrough and the low oil recovery from the flow rate bumps.

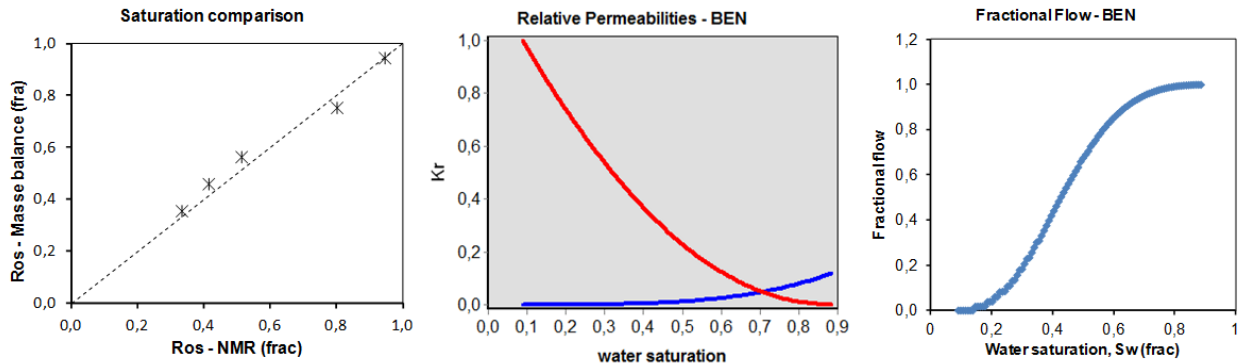


Figure 6 **Sireuil (left)**: comparison of remaining oil saturation determined by NMR and by mass balance from the flood effluent. **Bentheimer (right)**: the computed K_r curve and the water fractional flow.

CONCLUSION

Two unsteady-state waterflood experiments were performed on a low-field DRX spectrometer (MARAN DRX2-HF from Oxford Ltd) in an attempt to constrain the computation of relative permeabilities with the NMR derived saturation profiles within core at key stages of the waterflood. NMR, as a monitoring technique, has provided an evaluation of the remaining oil saturation at each flood stage (from T_2 distributions and saturation profiles). The gravimetric (considered as reference) and NMR saturation measurements agree within 5 saturation units (s.u) at maximum. Monitoring the T_2 distribution of the oil in the rock during the flooding experiment allowed evidencing that no wettability alteration occurred. This would be useful in the case of a low salinity water-flood, where an alteration of wettability during the flooding can be suspected.

Furthermore, the spatially resolved T_2 maps have allowed partitioning the porosity and determining oil saturation per pore size classes, on the bimodal Sireuil carbonate. Another interest of these 2D maps was to evidence the oil localization in space, in addition to the pore size class. For example, even if the oil saturation profile looked uniform on Sireuil carbonate at Sw_i , the spatially resolved T_2 experiment oil evidenced saturation gradients. This is specific to the pore size sensitivity of NMR and could not have been observed using X-ray technique. With the ability to monitor a waterflood regarding to the different pore size classes, the use of NMR (compared to traditional methods like X-ray techniques) could provide further understanding of flow mechanisms, especially in complex system such as carbonate. As the time-dependent flow data were continuously measured, the reliable in situ NMR saturation profiles before and after the waterflood were used to further constrain the computation of relative permeability on the Bentheimer sandstone. The acquisition of in situ NMR measurements at each flow stage on Sireuil carbonate opens the range of possibilities for improving the difficult K_r

computation on heterogeneous rocks by providing valuable information on the localization of the remaining oil (along the flow direction and by pore size).

ACKNOWLEDGEMENTS

For helpful discussions and advises, the authors thank particularly Pascal Clament, Stephane Drouilhet, Abbas Zerkoune and Cyril Caubit, petrophysical department of TOTAL. We also thank Philippe Larrieu and Luc Bamiere, TOTAL, for their assistance with the experiment setup.

REFERENCES

- [1] J. Heaviside and C. Black, "Fundamentals of Relative Permeability: Experimental and theoretical Considerations," in *SPE*, 1883.
- [2] C. McPhee and K. Arthur, "Relative Permeability Measurement: An Inter-Laboratory Comparison," in *SPE*, 1994.
- [3] C. McPhee, J. Reed and I. Zubizarreta, *Core Analysis: a Best Practice Guide*, Amsterdam: Elsevier, 2015.
- [4] A. Hove, J. Ringen and P. Read, "Visualization of Laboratory Corefloods with the aid of Computerized Tomography of X-rays," in *SPE*, 1987.
- [5] J. Mitchell, J. Edwards, E. Fordham, J. Staniland, R. Chassagne and P. Cherukupalli, "Quantitative Remaining Oil Interpretation Using Magnetic Resonance: From the Laboratory to the Pilot," in *SPE*, 2012.
- [6] R. Ramamoorthy, M. Kristensen, J. Edwards, C. Ayan and K. Cig, "Introducing the Micropilot: Moving Rock Flooding Experiments Downhole," in *SPWLA*, 2012.
- [7] S. Arora, D. Horstmann and P. Cherukupalli, "Single Well In-Situ Measurement of Residual Oil Saturation after an EOR Chemical Flood," in *SPE*, 2010.
- [8] A. Al-Yaarubi, J. Edwards, J. Guntupalli, L. Al-Qasmi, J. Kechichian, G. Al-Hinai and M. Appel, "Field Experience of NMR Logging Through Fiber-Reinforced Plastic Casing in an Observation Well.," in *SPWLA*, 2015.
- [9] K. Washburn and G. Madelin, "Imaging of multiphase fluid saturation within a porous material via ⁷ sodium NMR," *Journal of Magnetic Resonance*, 2010.
- [10] A. Shabib-Asl, M. Ayoub and K. Elrais, "Laboratory Investigation into Wettability Alteration by Different Low Salinity Water Compositions in Sandstone Rock," in *SPE*, 2015.
- [11] S. E. Buckley and M. C. Leverett, "Mechanism of Fluid Displacement in Sands," *SPE*, no. doi:10.2118/942107-G, 1942.
- [12] H. J. Welge, "A Simplified Method for Computing Oil Recovery by Gas or Water Drive," *SPE*, no. doi:10.2118/124-G, 1952.